

# Nanoscale

Accepted Manuscript



This is an *Accepted Manuscript*, which has been through the Royal Society of Chemistry peer review process and has been accepted for publication.

*Accepted Manuscripts* are published online shortly after acceptance, before technical editing, formatting and proof reading. Using this free service, authors can make their results available to the community, in citable form, before we publish the edited article. We will replace this *Accepted Manuscript* with the edited and formatted *Advance Article* as soon as it is available.

You can find more information about *Accepted Manuscripts* in the [Information for Authors](#).

Please note that technical editing may introduce minor changes to the text and/or graphics, which may alter content. The journal's standard [Terms & Conditions](#) and the [Ethical guidelines](#) still apply. In no event shall the Royal Society of Chemistry be held responsible for any errors or omissions in this *Accepted Manuscript* or any consequences arising from the use of any information it contains.

## ARTICLE

# Reduced graphene oxide-coated hydroxyapatite composites stimulate spontaneous osteogenic differentiation of human mesenchymal stem cells†

Cite this: DOI: 10.1039/x0xx00000x

Received 00th January 2012,  
Accepted 00th January 2012

DOI: 10.1039/x0xx00000x

[www.rsc.org/nanoscale](http://www.rsc.org/nanoscale)Jong Ho Lee,<sup>‡<sup>a</sup></sup> Yong-Cheol Shin,<sup>‡<sup>a</sup></sup> Oh Seong Jin<sup>a</sup>, Seok Hee Kang<sup>a</sup>, Yu-Shik Hwang<sup>b</sup>, Jong-Chul Park<sup>c</sup>, Suck Won Hong<sup>\*<sup>a</sup></sup> and Dong-Wook Han<sup>\*<sup>a</sup></sup>

Human mesenchymal stem cells (hMSCs) have great potentials as cell sources for bone tissue engineering and regeneration, but the control and induction of their specific differentiation into bone cells remain challenging. Graphene-based nanomaterials are considered attractive candidates for biomedical applications such as scaffolds in tissue engineering, substrates for SC differentiation and components of implantable devices, due to their biocompatible and bioactive properties. Despite the potential biomedical applications of graphene and its derivatives, only limited information is available regarding their osteogenic activity. This study concentrates upon effects of reduced graphene oxide (rGO)-coated hydroxyapatite (HAp) composites on osteogenic differentiation of hMSCs. The average particle sizes of HAp and rGO were  $1270 \pm 476$  nm and  $438 \pm 180$  nm, respectively. When coated on HAp particulates, rGO synergistically enhanced spontaneous osteogenic differentiation of hMSCs, without hampering their proliferation. This result was confirmed by determining alkaline phosphatase activity and mineralization of calcium and phosphate as early and late stage markers of osteogenic differentiation. It is suggested that rGO-coated HAp composites can be effectively utilized as dental and orthopedic bone fillers since these graphene-based particulate materials have potent effects on stimulating the spontaneous differentiation of MSCs and show superior bioactivity and osteoinductive potential.

## 1. Introduction

Graphene is defined as a one-atom thick, planar monolayer of carbon atoms arranged into a two-dimensional honeycomb crystal lattice.<sup>1</sup> As with many novel materials, applications of graphene and its family nanomaterials, such as graphene oxide (GO) and reduced GO (rGO), offer various technological opportunities since they exhibit exceptional electrical, thermal, optical and mechanical properties.<sup>2</sup> The practical uses of graphene and its derivatives are extensive, including applications as diverse as nanoelectronics (e.g. transistors and sensors), anti-bacterial paper and many biomedical uses such as drug delivery, imaging, theranosis and cytoprotection.<sup>3-8</sup> Recently, much attention has been paid to the potential of graphene-based materials as factors promoting osteogenic and neuronal differentiation of mesenchymal and neural stem cells, respectively.<sup>9-14</sup> Some studies, in particular, have endeavored to determine the behavioral changes of stem cells on a specific substrate coated or patterned with graphene or its derivatives. Other recent approaches aimed to enhance the differentiation of stem cells towards a specific lineage using 3D graphene foams are gaining attention.<sup>15,16</sup> However, compared to graphene-based substrates and foams, the bioactive potential of graphene-based composite particles remains unexplored. Most research dealing with graphene-based particles have focused on their biocompatibility, i.e., whether they are safe or toxic *in vitro* and/or *in vivo*.<sup>17-20</sup>

Bone morphogenetic protein-2 (BMP-2) or BMP-3 (osteogenin), vitamin D3,  $\beta$ -glycerophosphate and ascorbate are well known as osteogenic differentiation-inducing factors.<sup>21,22</sup> Among these osteoinductive agents, BMP-2 is the most potent morphogen inducing osteogenic differentiation from mesenchymal stem/progenitors. During several decades, BMP-2 has been widely applied for bone tissue engineering as well as for improved osseous integration of the bone/implant interface in various experimental animal models and clinical trials.<sup>23-26</sup> However, there has been critical concern that BMP-2 could cause bone to form outside the fusion area in places, known as ectopic bone formation, where it could be harmful since it is a powerful promoter of new bone growth.<sup>27-29</sup>

Here, we examine the effects of rGO-coated hydroxyapatite (HAp) composites on the osteogenic differentiation of human mesenchymal stem cells (hMSCs) and compare their effects between culture conditions with and without osteogenic inducers. Alkaline phosphatase (ALP) activity and mineralization of calcium and phosphate are determined as early and late stage markers of osteogenic differentiation of hMSCs grown in monolayer cultures. Immunocytochemistry and immunoblot analysis are performed to investigate the expression of osteogenic proteins including osteopontin (OPN) and osteocalcin (OCN), which are associated with matrix maturation and calcification, respectively.<sup>30</sup> Our results show that rGO-coated HAp composites stimulate osteogenesis in

hMSCs incubated in basal media (BM) in the absence of osteoinductive agents and osteogenic activity is further enhanced when those agents are added to culture media, defined as osteogenic media (OM). These observations, which could have general significance, demonstrate the potential of rGO-coated HAp composites to promote spontaneous osteogenic differentiation of hMSCs in the absence of any osteogenic inducers and growth factors.

## 2. Materials and methods

### 2.1. Synthesis of rGO nanoplatelets

GO was synthesized from expanded graphite using a modified Hummers and Offeman method.<sup>31</sup> As a starting material, a small amount of expandable graphite (Asbury Carbon, Grade 1721) was placed into a 500 mL beaker and heated for ~10 sec in a microwave oven; the expansion of graphite to ~150 times its original volume was induced. For the acid treatment process, a 250 mL flask, equipped with a Teflon-coated magnetic stirrer, was filled with 50 mM of concentrated sulfuric acid. The flask was then placed into an ice bath maintained at 0 °C. Subsequently, the expanded graphite (2 g) was added slowly to the flask to make a suspension, followed by the slow addition of potassium permanganate (6 g). The temperature was then increased to 35 °C, and the suspension was stirred for approximately 2 h. The flask was then placed in an ice bath to cool the mixture, and the excess deionized (DI) water was added slowly to the mixture, maintaining the temperature below 70°C. H<sub>2</sub>O<sub>2</sub> (30 wt%) was then added slowly to remove the potassium permanganate; vigorous bubbles appeared and the color of the suspension changed from dark brownish to yellow. The suspension was filtered several times and diluted with DI water to remove the acid completely; the pH of the dispersion was monitored until it reached 6. Finally, after suction drying over 12 h, the GO NPs were prepared. For the reduction process,<sup>32</sup> the synthesized GO (1 g) was sonicated in 1 L DI water for 2 h. Hydrazine hydrate (10 mL) was then added to the suspension and the reaction proceeded at 100°C for 24 h. After the reaction, the suspension was filtered and washed several times with water/ethanol solution. Finally, the rGO NPs were prepared after the drying in a vacuum oven at 80 °C for 12 h.

### 2.2. Preparation and characterization of rGO-coated HAp composites

A water-soluble calcium phosphate HAp powder (Bone Tech Inc., Miryang-si, Korea) was used to prepare the HAp microparticles. The qualitative and quantitative properties of the HAp powder had already been characterized by X-ray diffraction, inductively coupled plasma-optical emission spectroscopy and energy dispersive spectroscopy to corroborate that the prepared HAp powder was similar to natural HAp.<sup>33</sup> From these analyses, it was found that the weight percentage of CaO and P<sub>2</sub>O<sub>5</sub> in the HAp powder was 57.0 wt% and 41.4 wt%, respectively as well as the molar ratio of Ca and P was 1.67. The morphologies and average particle sizes of HAp microparticles and rGO nanoparticles (NPs) were characterized by field emission scanning electron microscopy (FESEM; Hitachi S-4700, Hitachi, Tokyo, Japan), atomic force microscopy (AFM; SPM-9600, Shimadzu, Tokyo, Japan) and a zetasizer (Malvern Instruments, Nano ZS, Worcestershire, UK).

To prepare the rGO-coated HAp composites, the HAp microparticles were suspended in DI water and mixed with a colloidal dispersion of rGO NPs at a 1:1 weight ratio. The mixed colloidal dispersion was vortexed vigorously for 10 min and the solvent was allowed to air-dry slowly overnight at room temperature, resulting in rGO-coated HAp composites. To eliminate residual rGO, the composites were washed three times with DI water. The morphology of the rGO-coated HAp composites was characterized by FESEM (Hitachi S-4700) at an accelerating voltage of 5 kV. Surface potentials and Raman spectra of HAp microparticles, rGO NPs and rGO-coated HAp composites were determined using a zetasizer (Malvern Instruments) and a Raman spectroscope (Micro Raman PL Mapping System, Dongwoo Optron Co., Ltd, Gwangju-si, Korea), respectively. While measuring the zeta-potential, the pH value of each suspension (10 µg mL<sup>-1</sup>) was monitored and kept at pH 7.0.

### 2.3. Cell proliferation assay

hMSCs were purchased from Lonza (Walkersville, MD) and used between passages 5 and 7. Cells were cultured in MSC BM (Lonza), supplemented with 10% MSC growth supplement, 2% L-glutamine and 0.1% GA-1000, containing a 1% antibiotic antimycotic solution (including 10,000 U penicillin, 10 mg streptomycin, and 25 µg amphotericin B per mL, Sigma-Aldrich Co.) at 37 °C in a humidified atmosphere of 5% CO<sub>2</sub>. Cell proliferation was measured by using a cell counting kit-8 (CCK-8, Dojindo, Kumamoto, Japan), which contains a highly water-soluble tetrazolium salt [WST-8, 2-(2-methoxy-4-nitrophenyl)-3-(4-nitrophenyl)-5-(2,4-disulfophenyl)-2H-tetrazolium, monosodium salt] reduced to a yellow-colour formazan dye by mitochondrial dehydrogenases. Typically, the hMSCs were seeded at a density of 1 × 10<sup>4</sup> cells mL<sup>-1</sup> in a 96-well plate and maintained in the media at 37 °C in an atmosphere containing 5% CO<sub>2</sub>. When seeding cells, the cell suspension was incubated with a colloidal dispersion of HAp microparticles, rGO NPs or rGO-coated HAp composites in BM at 10 µg mL<sup>-1</sup> and was then plated within 10 min and grown as monolayer cultures. After 1, 7, 14 and 21 days of incubation, cells were washed twice with Dulbecco's phosphate-buffered saline (DPBS, Sigma-Aldrich Co.) and then incubated with a WST-8 solution for 4 h at 37 °C under a 5% CO<sub>2</sub> atmosphere. To examine the effects of HAp microparticles, rGO NPs or rGO-coated HAp composites on the proliferation of hMSCs, the absorbance was measured at 450 nm using an ELISA reader (SpectraMax<sup>®</sup> 340, Molecular Device Co., Sunnyvale, CA). The cell proliferation profile was determined as the percentage ratio of the optical density in the cells (incubated with HAp microparticles, rGO NPs or rGO-coated HAp composites at each time point) to that in the non-treated control at 1 day.

### 2.4. ALP activity assay

Similar to the proliferation assay, the suspension of hMSCs was seeded in a 96-well plate and incubated with a colloidal dispersion of HAp microparticles (10 µg mL<sup>-1</sup>), rGO NPs (10 µg mL<sup>-1</sup>) or rGO-coated HAp composites (10 µg mL<sup>-1</sup>) in BM at 37 °C under a 5% CO<sub>2</sub> atmosphere. At the end of each pre-determined incubation period (1 to 21 days), cells were washed twice with DPBS and then incubated in Tris buffer (10 mM, pH 7.5) containing 0.1% Triton X-100 (Sigma-Aldrich Co.) for 10 min. An aliquot (100 µL) of each well was added to another

96-well plate containing 100  $\mu\text{L}$  of a  $p$ -nitrophenyl phosphate solution prepared previously using an alkaline phosphatase assay kit (Abcam, Cambridge, MA) at 37 °C.  $p$ -Nitrophenol, which is yellow in color, was produced in the presence of ALP and the absorbance was determined at 405 nm using an ELISA reader (Molecular Devices Co.). The absorbance vs. time plot was used to calculate the ALP activity of hMSCs treated with HAp microparticles, rGO NPs or rGO-coated HAp composites.

### 2.5. Alizarin red S staining

The Alizarin red S (ARS) stain was used to monitor the mineralization of the ECM by calcium accumulation. The suspension of hMSCs was seeded at a density of  $2 \times 10^5$  cells  $\text{ml}^{-1}$  in a 6-well plate, and incubated with a colloidal dispersion of HAp microparticles ( $10 \mu\text{g ml}^{-1}$ ), rGO NPs ( $10 \mu\text{g ml}^{-1}$ ) or rGO-coated HAp composites ( $10 \mu\text{g ml}^{-1}$ ) in BM at 37°C under a 5%  $\text{CO}_2$  atmosphere. After incubation for 1 to 21 days, the cells were washed twice with DPBS, fixed with 2% paraformaldehyde (Sigma-Aldrich Co.) and then stained with 40 mM ARS (pH 4.2, Sigma-Aldrich Co.). The culture plates were photographed under an optical microscope (Leica DMIL, Leica Microsystems, Wetzlar, Germany) with a digital camera (Olympus Optical Co., Osaka, Japan). The mineralized nodules are shown as a dark red center and light red peripheral area. For quantitative analysis, ARS in a stained monolayer of cells was extracted by adding a 10% acetic acid solution for 30 min with constant shaking and then neutralized with a 10% ammonium hydroxide solution, which was followed by colorimetric detection at 405 nm using an ELISA reader (Molecular Devices Co.).

### 2.6. Von Kossa staining

Von Kossa stain, which is not specific for calcium itself, but stains phosphates or carbonates in calcium deposits a brownish-blackish colour, was used to characterize the biological mineralization of the differentiated osteoblasts. The suspension of hMSCs was seeded at a density of  $2 \times 10^5$  cells  $\text{ml}^{-1}$  in a 6-well plate and incubated with a colloidal dispersion of HAp microparticles, rGO NPs or rGO-coated HAp composites at  $10 \mu\text{g ml}^{-1}$  in BM under a 5%  $\text{CO}_2$  atmosphere at 37 °C. After incubation for 1 to 28 days, the cells were washed twice with DPBS and fixed with 10% phosphate-buffered formalin for 10 min. The cells were then stained with a freshly prepared 5% silver nitrate solution for 30 min and washed three times with DI water. Subsequently, the cells were developed with fresh 5% sodium carbonate in 25% formalin for more than 5 min for mineral and matrix staining. After three washes with DI water, the cells were fixed with 5% sodium thiosulfate for 2 min to remove any unreacted silver nitrate. Finally, the cells were washed three times with DI water and air-dried, and photographs were taken using a digital camera (Olympus Optical Co.).

### 2.7. Immunocytochemistry

For immunofluorescence staining, the suspension of hMSCs was incubated with or without rGO-coated HAp composites ( $10 \mu\text{g ml}^{-1}$ ) for 14 days. After incubation, the cells were fixed with 4% paraformaldehyde (Sigma-Aldrich Co.) in DI water for 15 min at room temperature, permeabilized with 0.2% Triton-X in PBS and blocked with 10% goat serum (Sigma-Aldrich Co.)

with 0.05% Triton-X in PBS. Cells were incubated with primary antibodies overnight at 4 °C, incubated with secondary antibodies for 2 h at room temperature in the dark, and counterstained with propidium iodide ( $1 \mu\text{M}$ , Sigma-Aldrich Co.). Primary antibodies included rabbit monoclonal to OPN and mouse monoclonal to OCN (1:500 and 1:250 dilutions, respectively, Abcam). Secondary antibodies included DyLight488-conjugated goat anti-rabbit (1:500 dilution, Abcam) and DyLight488-conjugated goat anti-mouse (1:500 dilution, Abcam). All cells were imaged under a fluorescence microscope (IX81-F72, Olympus Optical Co.) and images were post-processed in ImageJ software.

### 2.8. Western blotting

After incubation with HAp microparticles, rGO NPs or rGO-coated HAp composites at  $10 \mu\text{g ml}^{-1}$  for 21 days, the hMSCs were washed twice with cold PBS (10 mM, pH 7.4) and ice-cold RIPA lysis buffer (Santa Cruz Biotechnology Inc., Santa Cruz, CA) was then added. After 5 min, the cells were scraped, and the lysate was centrifuged at  $14,000 \times g$  for 20 min at 4°C. The proteins were extracted from the total lysate, and the protein concentration was determined using a BCA™ protein assay according to the manufacturer's protocol (Pierce, Rockford, IL). For immunoblot analysis, equal amounts of protein ( $40 \mu\text{g}$ ) were run on a 4/20 polyacrylamide-SDS gel (Daiichi Pure Chemicals Co, Ltd, Tokyo, Japan) for 1 h at 30 mA and blotted onto a PVDF membrane for 50 min at 35 mA. The blots were blocked in a blocking buffer (Nacalai Tesque Inc., Kyoto, Japan) for 1 h at room temperature and incubated with the same antibodies to OPN and OCN, as used above at a 1:1,000 dilution. As a reference, mouse glyceraldehyde-3-phosphate dehydrogenase (GAPDH) monoclonal antibody (Abcam) was used at a 1:5,000 dilution overnight at 4°C. The blots were incubated with either goat anti-rabbit (Santa Cruz Biotechnology Inc.) or goat anti-mouse (Amersham Biosciences, Buckinghamshire, England) secondary antibody, horseradish peroxidase-conjugated at 1:2,000 dilution. Protein expression was detected using a Chemilumi-one chemiluminescent kit (Nacalai Tesque Inc.) and X-ray film (Fujifilm, Tokyo, Japan).

### 2.9. Statistical analyses

All variables were tested in three independent cultures for each *in vitro* experiment, which was repeated twice ( $n = 6$ ). The quantitative data is expressed as the mean  $\pm$  standard deviation (SD). Prior to statistical analysis, the data was tested for the homogeneity of variances using a Levene test. Multiple comparisons to detect the effects of rGO-coated HAp composites on the proliferation, ALP activity, calcium deposits and osteogenic protein expression of hMSCs were carried out using one-way analysis of variance (ANOVA, SAS Institute, Cary, NC), which was followed by a Bonferroni test when the variances were homogeneous and a Tamhane test when variances were not. A  $p$  value  $< 0.05$  was considered significant.

## 3. Results and discussion

### 3.1. Characterizations of rGO-coated HAp Composites

The morphology of HAp microparticles was shown to be irregular-shaped granules with much smaller particulates bound on their surface and their average particle size was measured as  $1270 \pm 476$  nm (Fig. 1A). Both large and small sheets were presented in rGO and the average size was  $438 \pm 180$  nm (Figs. 1B-1 and 1B-2). Most of rGO NPs existed as single or few layers and the thickness of the rGO layer was around 1.5 nm according to AFM images (Figs. 1B-3 and 1B-4).

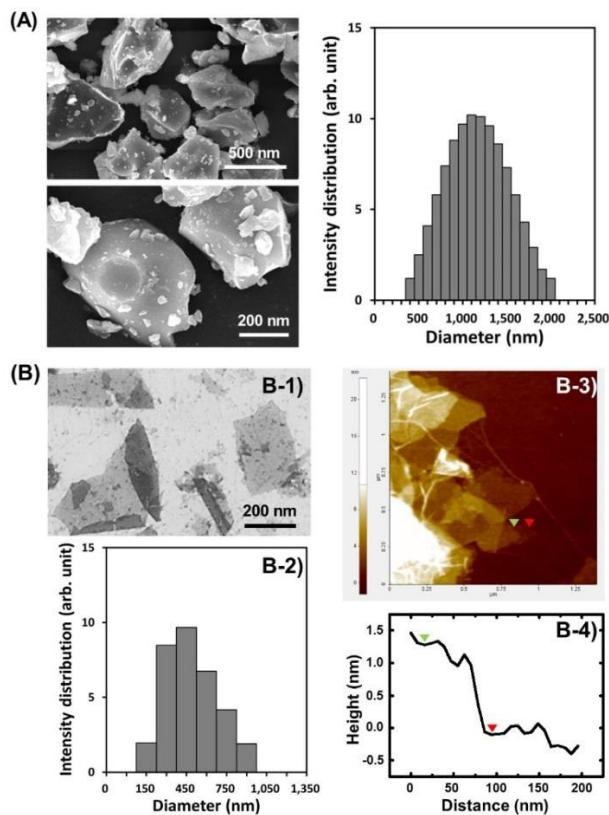


**Fig. 1** Morphology (by SEM), particle size distribution and/or topography (by AFM). (A) The morphology of HAp microparticles was irregular-shaped granules with much smaller particulates bound on their surface and their average particle size was  $1270 \pm 476$  nm. (B) Most of rGO NPs existed as single or few layers (B-1) with the average size of  $438 \pm 180$  nm (B-2). Both large and small sheets were mixed and the thickness of the rGO layer was around 1.5 nm (B-3 and B-4).

FESEM images show that HAp microparticles were partly wrapped and interconnected by an rGO network (Fig. 2A). A previous study reported that osteoblasts adhered well to and proliferated on GO/graphene-HAp hybrid materials, suggesting that they induce a 3D matrix adhesion of osteoblast cells with high cell viability and provide a similar microenvironment to that found *in vivo*.<sup>34</sup> The zeta potential analysis of surface potentials shows that rGO NPs in DI water (pH 7.0) were charged at about  $-34.5$  mV, whereas HAp microparticles were charged at about  $+6.5$  mV (Fig. 2B). It was shown that rGO NPs were negatively charged over a very wide pH range (0.5 ~ 10.0) and their zeta potential fluctuated between  $-30$  mV and  $-25$  mV after 6 h of hydrazine reduction or longer at pH 7.0.<sup>35</sup> A zeta potential  $>30$  mV (absolute value) is generally regarded as a critical value that represents sufficient mutual repulsion to guarantee the stability of a dispersion.<sup>36</sup> The surface charge of

rGO-coated HAp composites was measured to be around  $-23.7$  mV. These results indicate that rGO-coated HAp composites formed via electrostatic interactions between HAp microparticles and rGO NPs. Raman spectrum of rGO-coated HAp composites was dominated by several noticeable bands near at 430, 580, 960 and 1050  $\text{cm}^{-1}$ , which was due to the characteristic peaks of the phosphate groups abundant in HAp (Fig. 2C).<sup>37</sup> In addition, characteristic peaks of rGO were found near 1350  $\text{cm}^{-1}$  for the D band and at 1600  $\text{cm}^{-1}$  for the G band.<sup>38,39</sup> These characteristic peaks of HAp and rGO did not shift in rGO-coated HAp composites after coating. Therefore, it was confirmed that rGO NPs were firmly coated on the surface of HAp microparticles as shown in Fig. 2A.

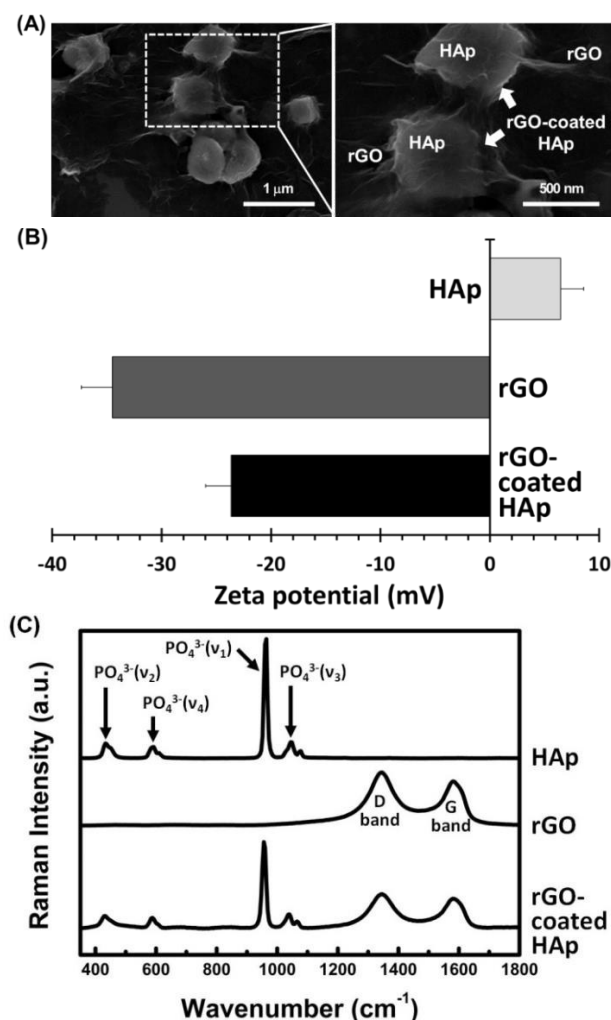


**Fig. 2** Physicochemical characteristics of rGO-coated HAp composites. (A) FESEM images of rGO-coated HAp composites showing rGO sheets surrounding HAp microparticles and covering the HAp MP surface. (B) Surface charges of HAp microparticles, rGO NPs and rGO-coated HAp composites indicating the formation of rGO-coated HAp composites via electrostatic interactions between HAp microparticles and rGO NPs. (C) Raman spectra of HAp microparticles, rGO NPs and rGO-coated HAp composites indicating that rGO NPs coat the HAp MP surface.

### 3.2. Cytotoxicity of rGO-coated HAp composites

In order to evaluate the cytotoxicity of HAp microparticles, rGO NPs and rGO-coated HAp composites, their effects on the metabolic activity of hMSCs were examined using a CCK-8 assay. We quantified the amount of the formazan dye, generated from WST-8 substrates by the activities of dehydrogenases in cells, as it is directly proportional to the number of living cells. As shown in Fig. S1†, cells exposed to increasing concentrations of HAp microparticles, rGO NPs and rGO-coated HAp composites for 24 h showed an appreciable dose-dependent decrease in the relative cell viability. HAp microparticles began to induce a significant ( $p < 0.05$ ) decrease in cell viability from  $31.3 \mu\text{g ml}^{-1}$ . The  $\text{IC}_{50}$  value of HAp microparticles was calculated to be about  $173 \mu\text{g ml}^{-1}$ , and they caused more than 55% loss of the cell viability at  $250 \mu\text{g ml}^{-1}$ . This cytotoxicity of HAp microparticles at relatively higher concentrations (over  $62.5 \mu\text{g ml}^{-1}$ ) might be partly explained by the intrinsic properties of alkaline HAp microparticles. A colloidal dispersion of HAp microparticles elevated the pH of culture media up to 7.97 and 8.20 (from 7.32) at 10 and  $100 \mu\text{g ml}^{-1}$ , respectively. Considering the *in vitro* cytotoxicity only, it seems that HAp microparticles can be safely used as particulate bone fillers at concentrations  $< 10 \mu\text{g ml}^{-1}$ . This result was consistent with that of another report.<sup>40</sup> On the contrary, rGO NPs and rGO-coated HAp composites demonstrated no significant decreases in cell viability at concentrations lower than  $62.5 \mu\text{g ml}^{-1}$ , and their  $\text{IC}_{50}$  values were expected to be approximately 517 and  $737 \mu\text{g ml}^{-1}$ , respectively. Particularly, the cytotoxicity of HAp microparticles was appreciably mitigated by coating them with rGO NPs. In recent comprehensive reports, it has been uncovered that neither obvious cytotoxicity nor significant cellular uptake of graphene and GO are shown in epithelial cells and macrophages at low concentrations (below  $50 \mu\text{g ml}^{-1}$ ) while higher concentrations could induce oxidative stress that slightly reduced the viabilities of cells.<sup>41,42</sup>

### 3.3. Effects of rGO-coated HAp composites on proliferation and ALP activity of hMSCs

Fig. 3A shows the effects of HAp microparticles, rGO NPs and rGO-coated HAp composites on the proliferation of hMSCs. At the first day of incubation, the addition of those particles to BM did not result in any reduction in cell proliferation, as compared to the non-treated control. Proliferation rates of cells incubated with rGO-coated HAp composites were slightly higher at 14 days than those of non-treated controls and cells incubated with HAp microparticles or rGO NPs. However, there was no significant difference among cells incubated with or without particles. After 21 days of incubation, cell proliferation was found to be nearly the same level as that seen in the non-treated control. These results imply that the initial exposure of particles to serum in the media did not adversely affect the proliferation of cell cultures. Even if the treatment concentration, cell type and culture condition were different from our study, there have been reported some contrasting results, demonstrating that when treated with relatively higher concentrations of HAp-rGO composites or cultured on HAp-rGO (or -GO) coatings, osteoblastic cells, such as hFOB 1.19, MC3T3-E1 and MG63 cells, showed better adherence and proliferation than non-treated cells or cells on non-coated surfaces.<sup>43-46</sup> This contrasting phenomenon might be explained by the hypothesis that could be attributed to the difference in physicochemical features including the composition ratio, particle size, surface charge, etc. of HAp-rGO composites. When hMSCs were

cultured in OM containing osteoinductive agents, such as  $\beta$ -glycerophosphate, dexamethasone and L-ascorbic acid,<sup>47,48</sup> the cell proliferation pattern was similar to that observed in the absence of those agents (Fig. S2A†). In this study, when seeding cells, the cell suspension was incubated with a colloidal dispersion of HAp microparticles, rGO NPs or rGO-coated HAp composites in BM until they were grown as monolayer cultures. This procedure was advantageous in that cells were initially exposed to rGO-coated HAp composites in 3D culture rather than as 2D plated monolayers and that the efficiency of cell contact with those composites was increased, which in turn facilitated intracellular signalling and subsequent osteogenic activity in hMSCs.<sup>49,50</sup>

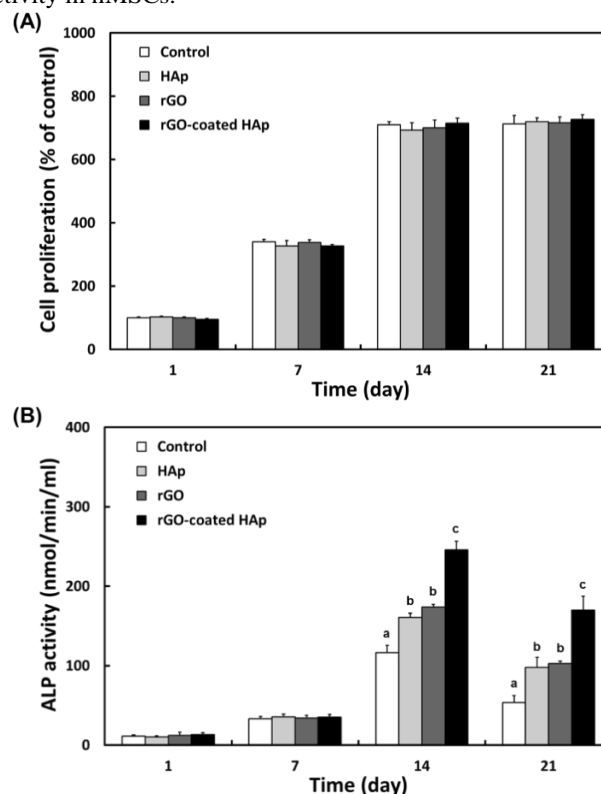


**Fig. 3** Proliferation and ALP activity of hMSCs incubated with a colloidal dispersion of HAp microparticles, rGO NPs or rGO-coated HAp composites in BM. (A) During the incubation period (up to 21 days), the presence of rGO-coated HAp composites resulted in no appreciable reduction in the cell proliferation, as compared to the non-treated control. (B) Incubation with rGO-coated HAp composites for 14 to 21 days significantly ( $p < 0.05$ ) induced ALP activity. The data is expressed as mean  $\pm$  SD based on at least duplicate observations from three independent experiments. The different letters denote significant differences between the non-treated control and cells incubated with particles,  $p < 0.05$ .

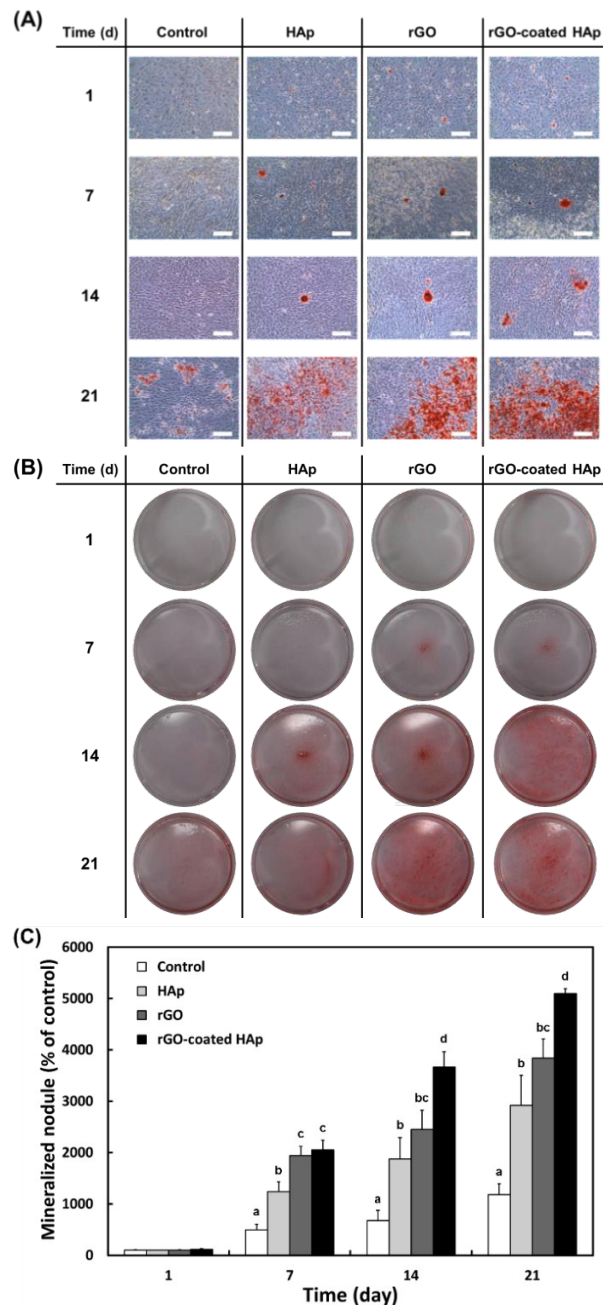
Cellular ALP activity did not show any consistent pattern correlated with cell proliferation (Fig. 3B), which could be due to the immediate secretion of ALP into media, since ALP is a secretory protein. Osteoblastic cells largely proliferate for up to 7 ~ 14 days and then start to secrete ECM proteins and produce early differentiation markers, such as ALP starting after 7 days.<sup>51</sup> When hMSCs were incubated with a colloidal dispersion of HAp microparticles, rGO NPs or rGO-coated HAp composites in BM without any osteogenic factors, it was not until day 7 that noticeable changes were observed. After 14

days of incubation with rGO-coated HAp composites, cells showed significantly ( $p < 0.05$ ) higher ALP activity than those incubated with either HAp microparticles or rGO NPs alone. These findings suggest that rGO-coated HAp composites can stimulate this early stage marker of osteoblast differentiation in the absence of any osteogenic factors. Various types of cells are known to exhibit an inverse relationship between growth and differentiation under *in vitro* conditions. In particular, some previous investigations of osteoblast developmental stages have indicated that as proliferation was retarded, differentiation markers, such as ALP activity and bone minerals, were increased.<sup>52,53</sup> Proliferating osteoblastic cells demonstrated a decreased expression of their typical phenotypic activities during periods of rapid growth as well. As cell replication slowed down, the cell began to produce more differentiation markers of an osteoblastic phenotype.<sup>33</sup> Furthermore, incubation with rGO-coated HAp composites even for 21 days was still potent in inducing ALP activity than incubation with either HAp microparticles or rGO NPs alone, indicating that HAp microparticles and rGO NPs act synergistically in osteoblast differentiation. In contrast, rGO NPs alone apparently induced ALP activity nearly up to the level of HAp microparticles alone. Some other reports have revealed that HAp-rGO (or -GO) composites substantially enhanced ALP activities of hFOB 1.19 and MG63 cells.<sup>54,55</sup> On the other hand, when cultured in OM, hMSCs showed remarkably higher ALP activity from day 7 than cells cultured in BM, regardless of the addition of particles (Fig. S2B†). At 14 days, ALP activities of hMSCs incubated with rGO NPs alone and rGO-coated HAp composites in OM reached up to 2.6 and 3.9 times their values in BM, respectively. The mixing ratio of HAp microparticles to rGO NPs had been predetermined and optimized - when reducing the content of rGO NPs by half (HAp : rGO = 1 : 0.5) or doubling their content (HAp : rGO = 1 : 2), rGO-coated HAp composites increased few, if any, ALP activity (Fig. S3(A)†). Additionally, the level of ALP activity of hMSCs incubated with rGO-coated HAp composites in 3D culture was superior to that in the 2D incubation system where the composites in BM was treated to as-grown monolayers of cells (Fig. S3B†).

### 3.4. Effects of rGO-coated HAp composites on calcium deposition and matrix mineralization in hMSCs

The image of ARS stain and its corresponding extract showed that rGO-coated HAp composites significantly ( $p < 0.05$ ) increased extracellular calcium deposition in hMSCs (Fig. 5). Increased calcium deposits by rGO-coated HAp composites were not related to the cell number as shown by the morphology using phase-contrast microscopy (Fig. 4A). There was a notable formation of calcium deposits by rGO-coated HAp composites from 14 to 21 days (Fig. 4B), indicating that HAp microparticles and rGO NPs synergistically induced calcium deposition in hMSCs. The dissolved ARS extracted from staining plates also confirmed the calcium staining pattern (Fig. 4C). Moreover, the calcium deposition in ECM formed by cells incubated with rGO-coated HAp composites resembled a fibrillar formation where calcium deposits in matrix were associated within the collagen fibrils, in contrast to the ARS staining of cells incubated under osteogenic conditions, which showed a diffuse granular appearance of calcium deposits (Figs. S4A† and S4B†). The ARS extract from cells cultured in OM almost agreed with the ALP activity profile (Fig. S4C†). These findings suggest that rGO-coated HAp composites have the capacity to induce an osteoid matrix deposition. In relation

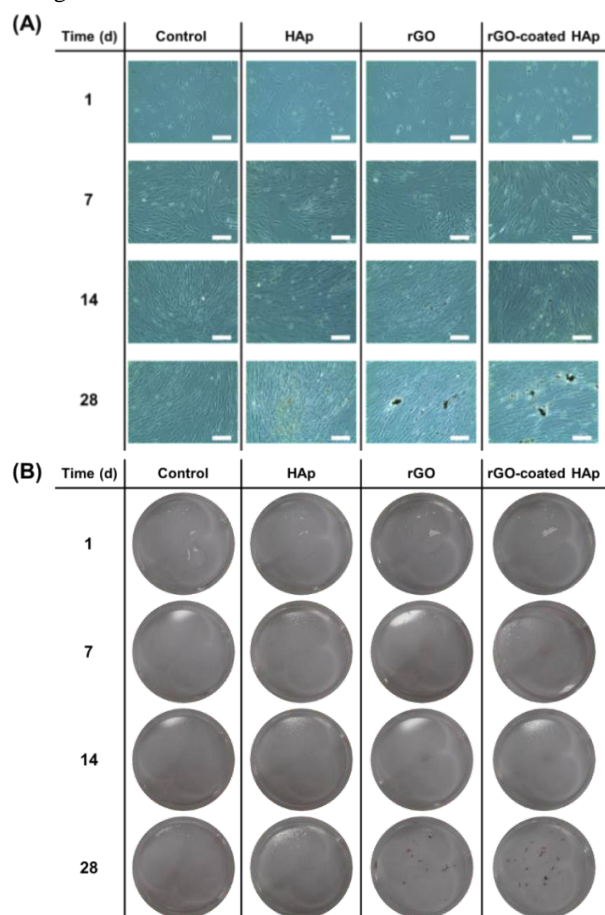
to our result, a recent study revealed that GO-calcium phosphate nanocomposites showed markedly synergistic effect in accelerating the osteogenesis of hMSCs by significantly increasing calcium deposition.<sup>56</sup> Compared with the 2D incubation system where a colloidal dispersion of HAp microparticles, rGO NPs or rGO-coated HAp composites in BM was treated to as-grown monolayers of hMSCs, the intensity of ARS staining was much highly enhanced in the 3D incubation system (Fig. S4D†).



**Fig. 4** ARS stain and its corresponding extract in hMSCs incubated with a colloidal dispersion of HAp microparticles, rGO NPs or rGO-coated HAp composites in BM. (A) Increased calcium deposits by rGO-coated HAp composites were not related to the cell number (scale bars = 200  $\mu$ m). (B) There was a notable formation of calcium deposits by rGO-coated HAp composites from 14 to 21 days indicating that HAp microparticles and rGO NPs synergistically

induce calcium deposition in hMSCs. (C) The dissolved ARS extracted from staining plates confirmed that rGO-coated HAp composites significantly ( $p < 0.05$ ) increased extracellular calcium deposition in hMSCs. The data is expressed as mean  $\pm$  SD based on at least duplicate observations from three independent experiments. The different letters denote significant differences between the non-treated control and cells incubated with any particles,  $p < 0.05$ . All photographs shown in this figure are representative of six independent experiments with similar results.

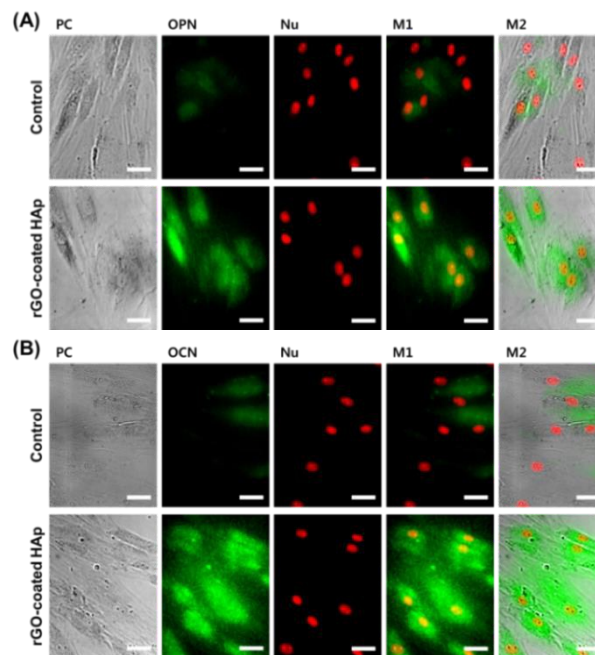
The image of von Kossa stain revealed that rGO-coated HAp composites significantly induced osteoblast differentiation with the formation of mineralized nodules by hMSCs (Fig. 5). Dark brown colored nodular staining could be observed on day 28 in hMSCs incubated with rGO-coated HAp composites (Fig. 5A), whereas there was little, if any, crystal formation in cells incubated with HAp microparticles alone (Fig. 5B). In addition, hMSCs incubated with rGO NPs alone exhibited strong positivity for von Kossa staining, confirming the formation of minerals in cells. Von Kossa staining was negative in control cultures without any particles. In the case of hMSCs cultured in OM, dark brown mineralized nodules and crystal formation were observed even at 21 days irrespective of the addition of particles (Figs. S5A† and S5B†). It has been shown that fibronectin-tethered GO on pure titanium substrates could play a potent role as an artificial matrix for osteogenesis by remarkably increasing mineralized matrices. These findings suggest that rGO-coated HAp composites can stimulate the marker for later osteogenic differentiation without the addition of osteogenic factors.<sup>57</sup>



**Fig. 5** Image of von Kossa stain in hMSCs incubated with a colloidal dispersion of HAp microparticles, rGO NPs or rGO-coated HAp composites in BM. (A) Dark brown coloured nodular staining was observed at 28 days in hMSCs incubated with rGO-coated HAp composites (scale bars = 200  $\mu$ m). (B) There was little, if any, crystal formation in hMSCs incubated with HAp microparticles alone, whereas cells incubated with rGO NPs alone exhibited strong positivity for von Kossa staining. Von Kossa staining was negative in control cultures without any particles. All photographs shown in this figure are representative of six independent experiments with similar results.

### 3.5. Effects of rGO-coated HAp composites on expressions of osteogenic proteins in hMSCs

Immunocytochemical analysis for osteogenic markers revealed that after 14 days of incubation in BM without any osteogenic factors, rGO-coated HAp composites appreciably upregulated the expression of OPN (Fig. 6A) and stimulated de novo expression of OCN in hMSCs (Fig. 6B). In contrast, non-treated cells showed few, if any, expression of both osteogenic markers. These data imply that rGO-coated HAp composites promote the spontaneous osteogenic differentiation of hMSCs. Our results are supported by very recent evidence demonstrating that graphene-cell biocomposites enhance pellet formation and differentiation of human bone marrow-derived hMSCs towards the chondrogenic lineage by preconcentrating growth factors.<sup>58</sup>



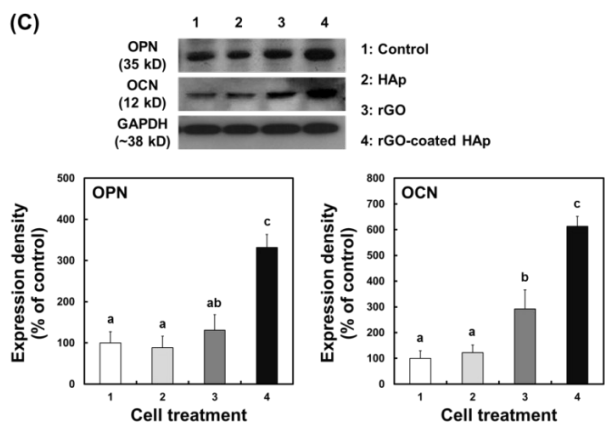


**Fig. 6** Immunostaining for osteogenic markers for hMSCs incubated with a colloidal dispersion of rGO-coated HAp composites in BM for 14 days. Culture of hMSCs with a colloidal dispersion of rGO-coated HAp composites stimulated de novo expression of the osteogenic markers OPN (A) and OCN (B) (scale bars = 20  $\mu$ m). These data confirm that rGO-coated HAp composites promote the spontaneous osteogenic differentiation of hMSCs. All photographs shown in this figure are representative of six independent experiments with similar results (PC: phase contrast, Nu: nucleus, M1: merge of OPN (or OCN) and Nu, M2: merge of PC and M1). (C) Immunoblotting for expressions of OPN and OCN in hMSCs incubated with a colloidal dispersion of HAp microparticles, rGO NPs or rGO-coated HAp composites in BM. After 21 days of incubation, the expression levels of both osteogenic proteins were significantly ( $p < 0.05$ ) increased by rGO-coated HAp composites. These results show good consistency with those of immunostaining (A and B) as well as ARS and von Kossa staining, other markers for late osteogenic differentiation. The data were expressed as mean  $\pm$  SD based on at least duplicate observations from three independent experiments. The different letters denote significant differences between the non-treated control and cells incubated with particles,  $p < 0.05$ .

Expressions of osteogenic proteins including OPN and OCN as markers of matrix maturation and mineralization, respectively were also assessed by an immunoblot analysis (Fig. 6C), which more confirmed the above qualitative immunostaining results. After 21 days of incubation, expression levels of both proteins in hMSCs were significantly ( $p < 0.05$ ) increased by rGO-coated HAp composites. rGO NPs alone were shown to appreciably increase expression of OCN as a matrix protein for calcification, whereas HAp microparticles alone did not greatly affect the expression of OPN and OCN. These results show good consistency with those of ARS and von Kossa staining, other markers for late osteogenic differentiation. A recent study has revealed that gelatin-functionalized GO can be efficiently used for the biomimetic mineralization of HAp, leading to promote the osteogenic differentiation of MC3T3-E1 cells.<sup>59</sup>

#### 4. Conclusions

In summary, we demonstrated that the osteogenic differentiation of hMSCs was enhanced by rGO-coated HAp composites when incubated in BM without any osteoinductive agents. In addition, we found that the osteogenic activity mediated by rGO-coated HAp composites was further enhanced when cells were cultured in OM. An initial exposure of cells to

a colloidal dispersion of rGO-coated HAp composites and subsequently increased contact with those composites, which in turn facilitated intracellular signalling, might be proposed as a feasible explanation. However, a more detailed mechanism, involving intracellular signal pathways, is yet obscure and requires further study at molecular levels. In any case, this work suggests that rGO-coated HAp composites can be potent factors in promoting the spontaneous osteogenic differentiation of osteoprogenitor cells as well as envisions that these rGO-based composites would be potential candidates for scaffolds in tissue engineering, stimulators for SC differentiation and components of implantable devices, due to their biocompatible and bioactive properties.

#### Acknowledgements

This work was supported by the Basic Science Research Program through the National Research Foundation of Korea (NRF) funded by the Ministry of Education, Science and Technology, Republic of Korea (2012R1A2A2A02010181).

#### Notes and references

- <sup>a</sup> Department of Cogno-Mechatronics Engineering, Pusan National University, Busan 609-735, Korea.
- <sup>b</sup> Department of Maxillofacial Biomedical Engineering, School of Dentistry and Institute of Oral Biology, Kyung Hee University, Seoul 130-701, Korea.
- <sup>c</sup> Cellbiocontrol Laboratory, Department of Medical Engineering, Yonsei University College of Medicine, Seoul 120-752, Korea.
- † Electronic Supplementary Information (ESI) available: Additional figures. See DOI: 10.1039/b000000x/
- ‡ The first two authors contributed equally to this work.
- 1 A. K. Geim and K. S. Novoselov, *Nat. Mater.*, 2007, **6**, 183-191.
- 2 V. Singh, D. Joung, L. Zhai, S. Das, S. I. Khondaker and S. Seal, *Prog. Mater. Sci.*, 2011, **56**, 1178-1271.
- 3 X. Huang, Z. Zeng, Z. Fan, J. Liu and H. Zhang, *Adv. Mater.*, 2012, **24**, 5979-6004.
- 4 W. Hu, C. Peng, W. Luo, M. Lv, X. Li, D. Li, Q. Huang and C. Fan, *ACS Nano*, 2010, **4**, 4317-4323.
- 5 Y. Zhang, T. R. Nayak, H. Hong and W. Cai, *Nanoscale*, 2012, **4**, 3833-3842.
- 6 J. L. Li, B. Tang, B. Yuan, L. Sun and X. G. Wang, *Biomaterials*, 2013, **34**, 9519-9534.
- 7 L. Feng, L. Wu and X. Qu, *Adv. Mater.*, 2013, **25**, 168-186.
- 8 H. K. Na, M. H. Kim, J. Lee, Y. K. Kim, H. Jang, K. E. Lee, H. Park, W. D. Heo, H. Jeon, I. S. Choi, Y. Lee and D. H. Min, *Nanoscale*, 2013, **5**, 1669-1677.
- 9 T. R. Nayak, H. Andersen, V. S. Makam, C. Khaw, S. Bae, X. Xu, P. L. Ee, J. H. Ahn, B. H. Hong, G. Pastorin and B. Özyilmaz, *ACS Nano*, 2011, **5**, 4670-4678.
- 10 W. C. Lee, C. H. Lim, H. Shi, L. A. Tang, Y. Wang, C. T. Lim and K. P. Loh, *ACS Nano*, 2011, **5**, 7334-7341.
- 11 S. Y. Park, J. Park, S. H. Sim, M. G. Sung, K. S. Kim, B. H. Hong and S. Hong, *Adv. Mater.*, 2011, **23**, H263-H267.
- 12 G. Y. Chen, D. W. Pang, S. M. Hwang, H. Y. Tuan and Y. C. Hu, *Biomaterials*, 2012, **33**, 418-427.

- 13 Y. Wang, W. C. Lee, K. K. Manga, P. K. Ang, J. Lu, Y. P. Liu, C. T. Lim and K. P. Loh, *Adv. Mater.*, 2012, **24**, 4285-4290.
- 14 A. Solanki, S. T. Chueng, P. T. Yin, R. Kappera, M. Chhowalla and K. B. Lee, *Adv. Mater.*, 2013, **25**, 5477-5482.
- 15 N. Li, Q. Zhang, S. Gao, Q. Song, R. Huang, L. Wang, L. Liu, J. Dai, M. Tang and G. Cheng, *Sci. Rep.*, 2013, **3**, 1604.
- 16 S. W. Crowder, D. Prasai, R. Rath, D. A. Balikov, H. Bae, K. I. Bolotin and H. J. Sung, *Nanoscale*, 2013, **5**, 4171-4176.
- 17 V. C. Sanchez, A. Jachak, R. H. Hurt and A. B. Kane, *Chem. Res. Toxicol.*, 2012, **25**, 15-34.
- 18 O. Akhavan, E. Ghaderi and A. Akhavan, *Biomaterials*, 2012, **33**, 8017-8025.
- 19 C. Bussy, H. Ali-Boucetta and K. Kostarelos, *Acc. Chem. Res.*, 2013, **46**, 692-701.
- 20 W. Shang, X. Zhang, M. Zhang, Z. Fan, Y. Sun, M. Han and L. Fan, *Nanoscale*, 2014, **6**, 5799-5806.
- 21 N. Z. Mostafa, R. Fitzsimmons, P. W. Major, A. Adesida, N. Jomha, H. Jiang and H. Uludağ, *Connect. Tissue Res.*, 2012, **53**, 117-131.
- 22 D. Zhou and Y. Ito, *RSC Adv.*, 2013, **3**, 11095-11106.
- 23 J. K. Park, J. -H. Shim, K. S. Kang, J. Yeom, H. S. Jung, J. Y. Kim, K. H. Lee, T. -H. Kim, S. -Y. Kim, D. -W. Cho and S. K. Hahn, *Adv. Funct. Mater.*, 2011, **21**, 2906-2912.
- 24 R. A. Thibault, A. G. Mikos and F. K. Kasper, *Adv. Healthcare Mater.*, 2013, **2**, 13-24.
- 25 L. D. Loozen, F. Wegman, F. C. Öner, W. J. A. Dhert and J. Alblas, *J. Mater. Chem. B*, 2013, **1**, 6619-6626.
- 26 Z. Su, J. Li, Z. Ouyang, M. M. L. Arras, G. Wei and K. D. Jandt, *RSC Adv.*, 2014, **4**, 14833-14839.
- 27 L. B. Shields, G. H. Raque, S. D. Glassman, M. Campbell, T. Vitaz, J. Harpring and C. B. Shields, *Spine*, 2006, **31**, 542-547.
- 28 E. J. Carragee, E. L. Hurwitz and B. K. Weiner, *Spine J.*, 2011, **11**, 471-491.
- 29 N. E. Epstein, *Surg. Neurol. Int.*, 2013, **4**, S343-S352.
- 30 G. S. Stein, J. B. Lian and T. A. Owen, *FASEB J.*, 1990, **4**, 3111-3123.
- 31 W. S. Hummers and R. E. Offeman, *J. Am. Chem. Soc.*, 1958, **80**, 1339.
- 32 S. Park, J. An, I. Jung, R. D. Piner, S. J. An, X. Li, A. Velamakanni and R. S. Ruoff, *Nano Lett.*, 2009, **9**, 1593-1597.
- 33 B. -K. Lim, F. Sun, S. -C. Ryu, K. Koh, D. -W. Han and J. Lee, *Biomed. Mater.*, 2009, **4**, 025017.
- 34 S. Kim, S. H. Ku, S. Y. Lim, J. H. Kim and C. B. Park, *Adv. Funct. Mater.*, 2011, **23**, 2009-2014.
- 35 M. Li, C. Liu, Y. Xie, H. Cao, H. Zhao, Y. Zhang, *Carbon*, 2014, **66**, 302-311.
- 36 D. H. Everett. *Basic Principles of Colloid Science*. London: The Royal Society of Chemistry; 1988.
- 37 C. Rodríguez-Valencia, M. López-Álvarez, B. Cochón-Cores, I. Pereiro, J. Serra and P. González P, *J. Biomed. Mater. Res. A*, 2013, **101**, 853-861.
- 38 G. Eda, G. Fanchini and M. Chhowalla, *Nat. Nanotechnol.*, 2008, **3**, 270-274.
- 39 Y. Zhou, J. Yang, T. He, H. Shi, X. Cheng and Y. Lu, *Small*, 2013, **9**, 3445-3454.
- 40 L. Wang, G. Zhou, H. Liu, X. Niu, J. Han, L. Zheng and Y. Fan, *Nanoscale*, 2012, **4**, 2894-2899.
- 41 A. Sasidharan, L. S. Panchakarla, A. R. Sadanandan, A. Ashokan, P. Chandran, C. M. Girish, D. Menon, S. V. Nair, C. N. Rao and M. Koyakutty, *Small*, 2012, **8**, 1251-1263.
- 42 K. Yang, Y. Li, X. Tan, R. Peng and Z. Liu, *Small*, 2010, **9**, 1492-1503.
- 43 L. Zhang, W. Liu, C. Yue, T. Zhang, P. Li, Z. Xing and Y. Chen, *Carbon*, 2013, **61**, 105-115.
- 44 M. Li, Q. Liu, Z. Jia, X. Xu, Y. Cheng, Y. Zheng, T. Xi and S. Wei, *Carbon*, 2014, **67**, 185-197.
- 45 Y. Liu, Z. Dang, Y. Wang, J. Huang and H. Li, *Carbon*, 2014, **67**, 250-259.
- 46 S. Baradaran, E. Moghaddam, W. J. Basirun, M. Mehrli, M. Sookhakian, M. Hamdi, M. R. Nakhai Moghaddam and Y. Alias, *Carbon*, 2014, **69**, 32-45.
- 47 E. Birmingham, G. L. Niebur, P. E. McHugh, G. Shaw, F. P. Barry and L. M. McNamara, *Eur. Cell. Mater.*, 2012, **23**, 13-27.
- 48 L. Kyllönen, S. Haimi, B. Mannerström, H. Huhtala, K. M. Rajala, H. Skottman, G. K. Sándor and S. Miettinen, *Stem Cell. Res. Ther.*, 2013, **4**, 17.
- 49 R. Gonzalez-McQuire, D. W. Green, K. A. Partridge, R. O. C. Oreffo, S. Mann and S. A. Davis, *Adv. Mater.*, 2007, **19**, 2236-2240.
- 50 L. A. Hails, J. C. Babister, S. Inglis, S. A. Davis, R. O. C. Oreffo and S. Mann, *Small*, 2010, **6**, 1986-1991.
- 51 G. S. Stein and J. B. Lian, *Endocrine Rev.*, 1993, **14**, 424-442.
- 52 L. D. Quarles, D. A. Yohay, L. W. Rever, R. Caton and R. Wenstrup, *J. Bone Miner. Res.*, 1992, **7**, 683-692.
- 53 H. Suh, D. -W. Han, J. -C. Park, D. H. Lee, W. S. Lee and C. D. Han, *Artif. Organs*, 2001, **25**, 459-466.
- 54 M. Li, Y. Wang, Q. Liu, Q. Li, Y. Cheng, Y. Zheng, T. Xia and S. Wei, *J. Mater. Chem. B*, 2013, **1**, 475-484.
- 55 Y. Liu, J. Huang and H. Li, *J. Mater. Chem. B*, 2013, **1**, 1826-1834.
- 56 R. Tatavarty, H. Ding, G. Lu, R. J. Taylor and X. Bi, *Chem. Commun.*, 2014, **50**, 8484-8487.
- 57 M. Nair, D. Nancy, A. G. Krishnan, G. S. Anjusree, S. Vadukumpully and S. V. Nair, *Nanotechnology*, 2015, **26**, 161001.
- 58 W. C. Lee, C. H. Lim, Kenry, C. Su, K. P. Loh and C. T. Lim, *Small*, 2015, **11**, 963-969.
- 59 H. Liu, J. Cheng, F. Chen, D. Bai, C. Shao, J. Wang, P. Xi and Zeng Z. *Nanoscale*, 2014, **6**, 5315-5322.